Evaluation of defect density in bulk gallium nitrides by photothermal deflection spectroscopy and steady-state photocapacitance methods

Masatomo Sumiya[1*], Hajime Fujikura[2], Yoshitaka Nakano[3], Shuhei Yashiro[1,4], Yasuo Koide[1], and Tohru Honda[4]

[1] *Next Generation Semiconductor Group, National Institute for Materials Science, Tsukuba, Ibaraki 305-0044, Japan*

[2] *Ibaraki Works, Sumitomo Chemical Co., Ltd., Hitachi, Ibaraki 319-1418, Japan*

[3] *Department of Electrical & Electronic Engineering, Chubu University, Kasugai, Aichi 487-8501, Japan*

[4] *Department of Applied Physics, School of Advanced Engineering, Graduate School of Engineering, Kogakuin University, 2665-1 Nakano, Hachioji, Tokyo 192-0015, Japan*

*Corresponding author. Email: SUMIYA.Masatomo@nims.go.jp

Abstract

Bulk GaN samples were characterized by both photothermal deflection spectroscopy (PDS) and steady-state photocapacitance (SSPC) methods. The PDS signal intensity in the bandgap was found to correlate quantitatively with the defect density estimated by the SSPC method. The defect density of GaN bulks fabricated by hydride vapor phase epitaxy (HVPE) was decreased by controlling the incorporating of carbon and silicon impurities. Differences in the reciprocal of the slope near the valence band maximum and the signal intensity in the bandgap among HVPE GaN bulks could be detected by PDS, although they had the same crystalline quality. PDS can be used to evaluate the GaN bulks that have been improved with a highly insulative property caused by Fe- doping or low carbon incorporation.

1. Introduction

Bulk GaN can be fabricated by several methods, including a high-pressure method,[1] hydride vapor phase epitaxy (HVPE),[2] an ammonothermal method,[3] or a Na-flux method.[4] Although free-standing bulk GaN substrates are available, their carrier density can be as high as ~10^{18} cm^{-3}. Since this indicates the presence of large numbers of defects such as vacancies or impurities, the improvement of bulk GaN is necessary for fabricating devices directly on bulk GaN substrates.

Over time, the crystallinity of bulk GaN has been gradually improved. The density of dislocations has been reduced to the order of 1×10^5 cm^{-2} by a hardness-controlled HVPE method.[5] The concentrations of carbon and Si impurities in bulk GaN have been reduced by changing the material of the reactor in HVPE.[6] The insulating properties of bulk GaN have been controlled by doping with C or Fe.[7] It is important to evaluate the defect levels and defect density in these improved bulk GaN samples. If the defect density in bulk GaN decreases further much lower, it will be more insulative, which indicates the difficulty of evaluating the defect density by electrical measurements.

We have applied photothermal deflection spectroscopy[8] (PDS) to evaluating the defect levels in the bandgap of III–V nitride materials.[9,10,11] The advantages of PDS are that an electrode on a sample is unnecessary and that electrically and/or optically inactive materials are available. This method can be used to evaluate the absorption coefficient of a semiconductor by detecting the heat generated by the nonradiative recombination of electrons excited by irradiating monochromatic light. When the absorption coefficient in the bandgap is ~10^2 cm^{-1}, the PDS can probe the depth of ~100 μm. We considered that

the PDS signal intensity in the bandgap could be increased for thick samples in the case of materials with low absorption coefficients such as bulk GaN, compared with deep-level transient spectroscopy (DLTS) the region of a depletion layer and positron annihilation spectroscopy (PAS)[12] detecting a depth of ~1 μm from the surface.

PDS is one of the established methods for evaluating the defect density in the bandgap of hydrogenated amorphous silicon (a-Si:H) film.[13] The density of states (DOS) in the bandgap was attributed to the defects of Si dangling bonds, and it was estimated from the relationship between the absorption coefficient and the defect density determined by electron spin resonance. There are several types of defects in III–V nitrides such as Ga or N vacancies, impurities, and dislocations that form each defect level in the bandgap. The identification of the origin of each defect level in III–V nitride semiconductors has still been controversial, and it is difficult to obtain the defect density in each defect level, especially in the middle of the bandgap.

To estimate the defect density in III–V nitrides quantitatively by PDS, we focused on the steady-state photocapacitance[14,15] (SSPC) method, which can be used to determine defect levels and their density quantitatively. During the SSPC measurement, the defect levels in the bandgap are fully occupied by electrons when applying the forward bias in the dark. After that, the reverse bias is applied in the dark. Electrons trapped in shallow defect levels are emitted to the conduction band. Electrons trapped in deep defect levels are excited to the conduction band by irradiating monochromatic light. The variation of capacitance caused by the incident photon energy indicates the defect density. By sweeping the incident photon energy up to the bandgap energy, we repeat these steps to obtain the defect levels and their density in the bandgap. The SSPC spectrum reflects the

integration of DOS in the bandgap. The PDS spectrum is also composed of the integrated DOS[16]. Both methods for III–V nitride semiconductors can be used to detect the defect levels close to the valence band,[9] whereas DLTS can be used to detect the defect levels close to the conduction band. We considered that the defect density of III–V nitride can be quantitatively estimated from the PDS signal intensity, in comparison with the value determined by the SSPC method.

In this study, we evaluated (1) free-standing GaN substrates fabricated by various methods by PDS to demonstrate the potential use of PDS, (2) bulk GaN and GaN films grown on it to obtain the correlation between the defect density evaluated by SSPC and the PDS signal intensity, and (3) a series of improved bulk GaN fabricated by Sumitomo Chemical Co.Ltd. by using both PDS and SSPC. By comparing the PDS and SSPC spectra, we determined whether the PDS signal intensity in the bandgap quantitatively corresponded to the defect density.

2. Experiment

2.1 Bulk GaN samples

Table 1 lists the samples in this study. The samples evaluated in this study were three categories. The first category was the free-standing *c*-plane (Ga-face: +*c*) GaN bulks (thickness: ~400 μm) prepared by various methods (HVPE, ammonothermal, or Na-flux) in several groups. The second category was *m*-plane GaN bulk substrate and GaN films (~5 μm) with lower carrier density (Si dope: 2×10^{16} cm^{-3}) grown on +*c* GaN substrate. These samples were measured by both PDS and SSPC measurements. The third category

was bulk GaN samples (200~400 µm) grown by HVPE in Sumitomo Chemical Co. Ltd.

Table 1 List of GaN samples

Sample#		method	Thickness (µm)	Carrier density or impurity (cm^{-3})	Dislocation density (cm^{-2})
AMT1	+c GaN bulk	Ammonothermal	518	$\sim10^{19}$	-
AMT2	+c GaN bulk	Ammonothermal	350	1×10^{19}	-
HVPE1	+c GaN bulk	HVPE	282	2.3×10^{18}	-
HVPE2	+c GaN bulk	HVPE	300	1.6×10^{18}	1.9×10^{6}
Na-flux1	+c GaN bulk	Na-flux	1500	O $<10^{17}$	10^{3}-10^{6} (EPD)
HVPE3	+c GaN bulk	HVPE	280	2.5×10^{18}	-
mHVPE4	m GaN bulk	HVPE	393	2.0×10^{18}	-
MOCVD1	GaN film on +c GaN bulk	MOCVD	5	2×10^{17}	-
HVPE5	+c GaN bulk	HVPE	414	1.2×10^{18}	2.6×10^{6}
HVPE6	+c GaN bulk	HVPE	200	2.0×10^{15} Si: 5e14 C: 3.8e14 O: <5e14	$\sim10^{6}$
HVPE7	+c GaN bulk	HVPE	450	1.2×10^{15} Si: 1.5e14 C: 1.4e14 O: 2.1e14	$\sim10^{6}$
HVPE8	+c GaN bulk	HVPE	342	Not detectable Fe:1e16, Si:5e14 C:1e15 O:<4e 14	$\sim10^{6}$

2.2 PDS measurement

In PDS method, the heat generated by nonradiative recombination was detected from the

deflection of a probe laser beam (660 nm) parallel to the surface of the sample which was placed in quartz cell filled with fluorinate solution inert chemically to GaN. The sample surface was irradiated with monochromatic light from an ozone-free solar simulator (Xe lamp) as a pumping source at a normal angle with a chopping frequency of 11 Hz. The pumping light was focused through a cylindrical lens with dimensions of 10 × 1 mm^2. The scan direction was from high to low photon energy. The position of deflected probe laser (PDS signal) was detected as a function of the energy of irradiated light. The photothermal deflection spectrum was obtained by normalizing the PDS signal intensity at the incident photon energy corresponding to the bandgap, because a few percent of electrons were contributed to the emitting light at room temperature. More details and difficulties in PDS for III–V nitride semiconductor are described in Refs. 9–11.

2.3 SSPC measurement

Capacitance–voltage (C–V) and SSPC measurements were performed at a frequency of 10 kHz with an ac modulation level of 50 mV using a Hg probe system in a lateral dot-and-ring Schottky-barrier-diode (SBD) configuration. The Schottky metal dot was 514 μm in diameter. Typical *n*-type rectifying characteristics in C–V measurement was carried out in the dark, and then we conducted SSPC studies, measuring the photocapacitance transients as a function of the incident photon energy from 0.78 eV (1600 nm) to 4.1 eV (300 nm). The SBDs were illuminated from the rear by concentrated monochromatic-light from a 250 W halogen lamp coupled with a high-resolution monochromator. The measurement bias voltage V_G was set at –3.0 V. In this study, the SSPC signal was defined as $2|N_D - N_A|\Delta C/C_0$, where $|N_D - N_A|$ is the effective carrier concentration determined from the C–V measurements at V_G = –3.0 V, C_0 was the

capacitance at a V_G of –3.0 V before optical excitation, and ΔC was the total photocapacitance variation, determined from the saturation value of the transients recorded at each incident photon energy. It took 300 sec long enough to obtain the saturated value for one data point. The variation in $2|N_D - N_A|\Delta C/C_0$ between the optical onset and the saturation positions of the deep-level defects in the SSPC spectra corresponds to the defect concentration.[17] The uncertainty of by SSPC system was 4% error for the capacitance measurement set-up, and the defect density determined by SSPC was the net concentration of defect.[18,19]

3. Results and discussion

3.1 PDS spectra for free-standing GaN substrates

Figure 1 shows the PDS spectra of free-standing bulk GaN samples fabricated by various methods. The Urbach-like energy (the reciprocal of the slope near the valence band maximum (VBM, E_v) and the PDS signal intensity in the bandgap were dependent on the growth method and the manufacturer. Several peaks were observed in the bandgap. The peak [defect level 1 (DL1)] was observed at the photon energy of around 2.6 eV from the VBM. Moreover, a broad peak at 2.2–2.4 eV, corresponding to the photon energy of yellow luminescence (YL) and green luminescence (GL), was observed in the PDS spectra.

Oxygen was usually incorporated as an impurity in ammonothermal bulk GaN (carrier density of ~10^{19} cm^{-3}), which appeared yellow, indicating that the absorption coefficient in the bandgap was high. Therefore, the PDS signal intensity in the bandgap tended to be

higher (~0.4) as shown in Fig. 1. Several additional impurities were incorporated into Na-flux bulk GaN, which generally appeared dark gray.[20] However, the intensity in the bandgap was much lower for the transparent area of Na-flux bulk GaN with low carbon impurity[21] analyzed selectively by PDS. The Xe lamp has the emission line at the wavelength of around 2.6–2.7 eV marked as DL1. Since there was no peak corresponding to DL1 in the Na-flux GaN sample, the influence of the emission line from the Xe lamp on the PDS spectrum was eliminated by dividing the PDS intensity by the incident photon flux. The peak at 2.7 eV was not an experimental error but the signal from the GaN sample.

The free standing GaN substrates (carrier density of 10^{18} cm^{-3}) fabricated by HVPE were transparent over their entire area. The defect level at 2.6 eV corresponding to E_v+~0.9 eV was reported to be an H1 hole trap.[22] The broad peak of PDS spectrum at 2.6 eV covered the defect levels of the H1 hole trap previously reported from 0.86 eV[23] to 0.94 eV[24] above the VBM. Distinct peaks in the spectra at 2.6 eV assigned to H1 defects can only occur if they are caused by a resonant transition between two distinct defect levels, not by defect-band transitions.[22] The cross section of electrons at the H1 hole trap was too small ($<\sim 10^{20}$ cm^2)[25,26] to cause the recombination. The nonradiative recombination may hardly occur through the H1 hole trap, indicating that no H1 hole trap was detected by PDS.

PDS may have the potential to detect defect levels in the mid-gap with high sensitivity. It is possible to detect the PDS signal between defect levels having an energy difference corresponding to the photon energy, especially for wide-bandgap semiconductors. It does not directly indicate the energy level from the bottom of E_c, but rather the energy difference between defect levels. This is one of the difficulties in PDS analysis as

mentioned in a previous report [27].

PDS signal intensities for photon energies lower than 1.8 eV were likely to increase in transparent bulk samples except for AMT1. The gradual increase was possibly contributed by the optical absorption coefficient from phonon-assisted free carrier absorption.[28] However, the actual increase shown in Fig. 1 seemed to be much larger than the reported experimental results.[29] The probing depth of the PDS measurement was the range of 1–10 μm determined using the absorption coefficient (10^4–10^3 cm^{-1}). [30] Defects extending across the depth of the bulk sample, such as dislocations observed at 1.6 eV by high-temperature DLTS, [31] might act as nonradiative recombination centers to increase the PDS signal intensity at around 1.6 eV. However, since we did not yet confirm the reason for the increase, the PDS application was limited up to the photon energy of 1.8 eV as described in the next sections. Here, it is worth noting that the difference in the Urbach-like energy and the intensity in the bandgap could be detected by PDS for two transparent HVPE samples with the same crystalline quality.

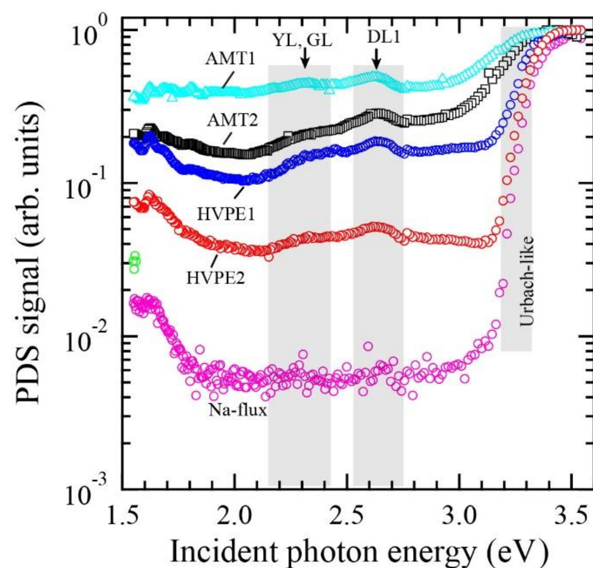

Fig. 1 PDS spectra of free-standing bulk GaN substrates manufactured by several methods.

3.2 Comparison between SSPC and PDS spectra

To obtain a quantitative estimation of defect density, we measured +c GaN bulks, an *m*-GaN bulk, and a GaN epilayer grown by MOCVD on bulk +c GaN by SSPC as shown in Figs. 2(a) and 2(b). The broad peak in the bandgap was composed of several peaks. They were difficult to distinguish, because it was hard to detect the variation of capacitance in the depletion layer for the sample with a high carrier density by SSPC. The defect density of +c GaN (blue) at around 2.6 eV was estimated to be 5.0×10^{16} cm^{-3} from the difference from the baseline (density of $0.6{\times}10^{17}$ cm^{-3} at 1.5 eV) in the SSPC spectrum shown in Fig. 2(a). The variations of the SSPC spectrum for bulk *m*-GaN (red) in the bandgap seemed to be small in Fig. 2(a). The defect density of bulk *m*-GaN (red) at 2.6 eV was estimated to be $2.7{\times}10^{16}$ cm^{-3}. For the GaN epilayer in Fig. 2(b), the SSPC spectrum indicated the sharp structures near the valence band, and the defect density of $1.6{\times}10^{15}$ cm^{-3} at 2.6 eV, which was lower by approximately one order of magnitude than those in Fig. 2(a), corresponding to the Si doping concentration (the carrier density).

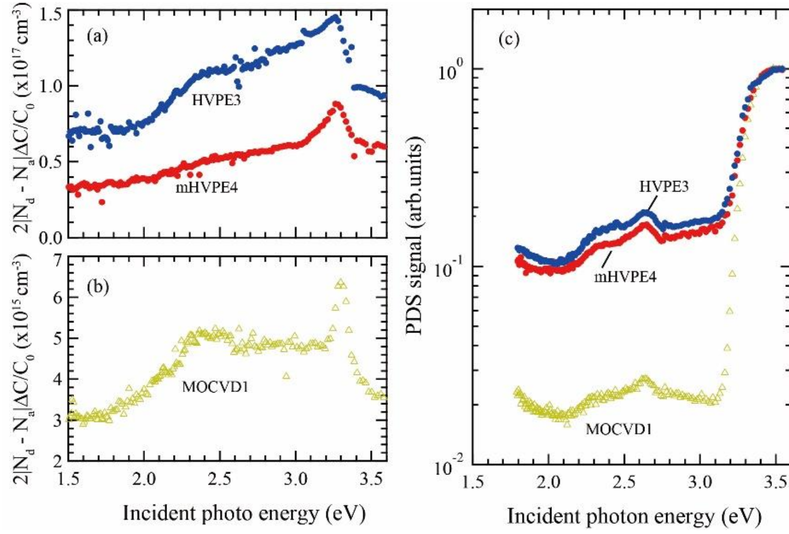

Fig. 2 (a) SSPC spectra for +c bulk GaN (Si doping: 2.5 × 10^{18} cm^{-3}) and, bulk m-GaN (Si doping: 2.0 × 10^{18} cm^{-3}), and (b) SSPC spectrum for a GaN epilayer (5 µm, Si doping: 2.0 × 10^{17} cm^{-3}) grown on +c bulk GaN by MOCVD. (c) PDS spectra for the same samples represented by the same color.

To compare the SSPC spectra, we measured the same samples by PDS as shown in Fig. 2(c) represented by the same color. The GaN epilayer on the GaN bulk was 5 µm thicker than the penetration depth in the PDS measurement. Judging from the PDS intensity, which is lower by two orders of magnitude than that at the bandgap energy, the penetration depth in the mid-gap energies was approximately from 1 to 10 µm. The incident monochromatic light penetrated to the depth comparable to the thickness of GaN epilayer. This is the reason why the PDS signal for the GaN epilayer was no influence from the underlying GaN bulk. When hetero or accumulated structures such as AlGaN/InGaN on the various substrates (GaN, Si or SiC) are evaluated by PDS, the signal from the layer with the smallest bandgap or the most defective layer tends to be dominant. This is another drawback of PDS.

PDS can detect the peaks clearly at 2.6 eV and 2.4 eV–2.2 eV in the bandgap. It was considered that this higher sensitivity was attributed to the detection depth. While the depth region was the depletion layer for SSPC, the long wavelength light corresponding to the inside bandgap penetrated into a depth of 1–10 μm as discussed in Sec. 3.1.

The signal intensity of the PDS spectra in the bandgap was found to decrease with the decrease in the defect density evaluated by SSPC. For the GaN epilayer, the PDS intensity in the bandgap was decreased to ~0.02, much lower by one order of magnitude, which was consistent with the quantitative evaluation by SSPC. No carrier distribution in the deletion layer was confirmed from the CV measurements. By assuming that the distribution of nonradiative recombination centers in the depletion layer was homogeneous throughout the entire sample, we compared the PDS spectra with the SSPC spectra to quantitative analyze the defect density. We plotted the relationship between the defect density evaluated by the SSPC and the PDS intensity at 2.2 and 2.6 eV in Fig. 3. The defect density determined by SSPC corresponded to the PDS signal intensity, indicating that the PDS intensity was associated with the defect density.

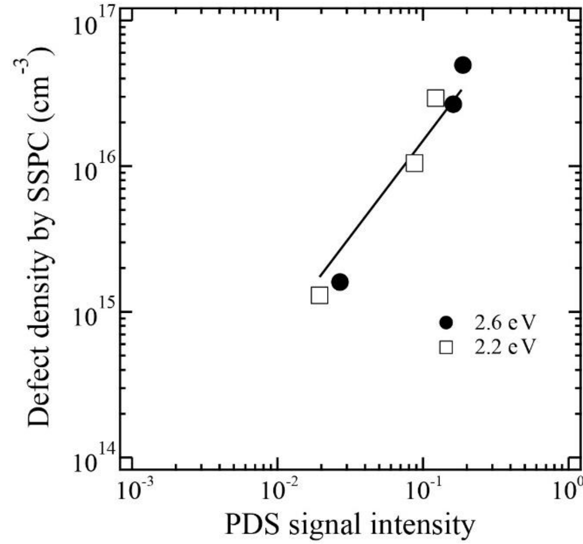

Fig. 3 Relationship between the defect density evaluated by SSPC and the PDS intensity at 2.6 (closed circle) and 2.2 eV (open square). The line is a guide for the eye.

3.3 PDS spectra for insulative bulk GaN samples

Figure 4 shows the PDS spectra of a series of +c bulk GaN samples commercialized (HVPE5 in Fig. 4) and improved (Refs. 6 and 7) by Sumitomo Chemical Co. Ltd. The PDS signal intensity at 2.6 eV was 4.5×10^{-2} for the conventional GaN bulk, and the defect density estimated by SSPC was about 1×10^{16} cm^{-3}. The PDS signal intensity for HVPE6 with a carbon concentration of 3.8×10^{14} cm^{-3} (fabricated in 2019) was ~10^{-2} in the bandgap, and the Urbach-like energy was 34 meV. When the carbon concentration was further reduced in 2020,[6] the quality of the bulk GaN was further improved. The Urbach-like energy was 29 meV and the signal intensity in the bandgap was less than 10^{-2}. Furthermore, the PDS signal intensity at 2.6 eV was reduced for HVPE7 with a carbon concentration of 1.0×10^{14} cm^{-3}. The result was consistent with a previous paper that showed that HVPE GaN bulks with a low carbon concentration fabricated by Sumitomo

Co. Ltd. had a low defect density at E_V+0.87 eV.[32] In 2021, while the technological level of reducing the concentration of carbon impurity was maintained, Fe atoms were additionally doped to improve the insulating properties of the bulk GaN.[7] The corresponding PDS signal intensity in the bandgap of HVPE8 was reduced to 10^{-3} or less, and that at 2.6 eV was markedly reduced.

Although doping with Fe increased the amount of the impurities of C, O and Si (no detection of the other impurities) by several times as listed in Table 1, the PDS intensity at 2.6 eV decreased as shown in Fig. 4. This behavior indicated that the defect level at 2.6 eV detected by PDS was not related to the carbon impurity at the N site (C_N) which is regarded as the origin of H1 hole trap. As discussed in Sec. 3.1, no H1 hole trap, $(V_{Ga}–Si)^{2-}$ of which was regarded as a candidate, was detected by PDS. The other possible impurity was oxygen. To the best of our knowledge, the defect level corresponding to 0.8 eV above the VBM was the H4 hole trap of -/0 charge state transition of the V_{Ga}–O complex.[33] However, nonradiative recombination hardly occurred at the hole trap. It is reasonable to consider that the density of intrinsic defects of V_{Ga} and/or V_N must be reduced in the state-of-the-art HVPE GaN bulk according to the yearly improved growth techniques. Consequently, we assumed that the PDS intensity at 2.6 eV might be reduced even for Fe-doped GaN bulk.

The defect level related to Fe impurities has been reported to be located at 0.5–0.6 eV under the bottom of the conduction band.[34,35] Wickramaratne et al. calculated the nonradiative recombination of the excited states of Fe^{3+} at 0.64 eV below the CBM and Fe^{2+} at 0.58 eV above the VBM in GaN.[36] There was no absorption of photon energy between the two levels due to the spin-conserving intradefect relaxation. These

calculation results were considered the reason why the defect levels related to the doped Fe were hardly detected in the PDS spectrum. It is still very difficult to determine the origin of the defect levels in the GaN bulk and related materials, although the plateau at 2.8–2.9 eV might be related to the state of Fe^{2+}, which should be investigated further.

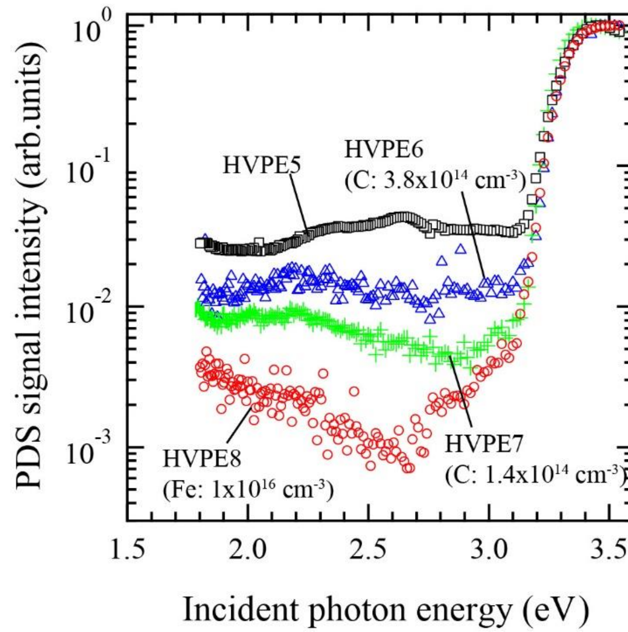

Fig. 4 PDS spectra for samples of bulk GaN grown by HVPE at Sumitomo Chemical.

The SSPC measurements were performed on these samples. Except for HVPE5, the other samples could not be measured by SSPC owing to their high insulating properties. One of the features of PDS is that it can be used to observe the defect levels in the bandgap of highly insulative semiconductors. By taking the PDS signal intensity of ~0.01 at 2.6 eV for HVPE6 (C: 3.8×10^{14} cm^{-3}) into account, we estimated that the in-gap defect density might be ~1×10^{15} or less cm^{-3} from Fig. 3. Other samples of HVPE7 with a low carbon (1.4×10^{14} cm^{-3}) sample and an Fe-doped HVPE8 sample, which exhibited lower PDS

signal intensities in the bandgaps of 4×10^{-3} and 1×10^{-3} at 2.6 eV, were considered to have much lower densities of defects of ~4×10^{14} and ~1×10^{14} cm^{-3}, respectively.

The detection limit of PAS was Ga vacancy-type defects of~10^{15} cm^{-3}.[37] If GaN bulk growth technology progresses and the in-gap defect density is reduced to the order of 10^{14} or 10^{13} cm^{-3}, it will become more difficult to evaluate the defect density in the band gap electrically owing to the higher resistivity of wide bandgap materials. PDS may be useful for the evaluation of defects in an insulative bulk GaN.

4. Summary

Bulk GaN samples grown by various methods were evaluated by PDS. For the transparent bulk GaN substrates fabricated by HVPE, PDS detected the differences with respect to the Urbach-like energy and the intensity in the bandgap. It was difficult to determine the absolute defect level, the origin of defect, and the defect density by PDS. For the attempt to estimate the defect density by PDS, the obtained PDS spectra were compared with the SSPC spectra for the same samples. There was a correlation between the defect density in the bandgap measured by SSPC and the PDS signal intensity. The defect density of ~1×10^{14} cm^{-3} in the bandgap was evaluated by PDS for highly insulative HVPE-GaN bulks. PDS has the potential for evaluating the insulative bulk GaN with the defect density and defect levels of ~1×10^{14} cm^{-3} order in the bandgap.

Acknowledgment

This study was partially supported by the Ministry of Education, Culture, Sports, Science

and Technology, Japan “Program for research and development of next-generation semiconductor to realize energy-saving society”.

References

[1] I. Grzegory, M. Bockowski, B. Lucznik, S. Krukowski, M. Wroblewski, S. Porowski, MRS Internet Journal of Nitride Semiconductor Research **1**, 18d (1996).

[2] Y. Oshima, T. Eri, M. Shibata, H. Sunakawa, K. Kobayashi, T. Ichihashi, and A. Usui, Jpn. J. Appl. Phys. **42**, L1 (2003).

[3] Hashimoto, T., Fujito, K., Saito, M., Speck, J.S., Nakamura, S., Jpn. J. of Appl. Phys., Part 2: Letters **44**, L1570 (2005).

[4] M. Yano, M. Okamoto, Y. K. Yap, M. Yoshimura, Y. Mori and T. Sasaki, Japanese Journal of Applied Physics, Part 2: Letters **38**, L1121 (1999).

[5] H. Fujikura, T. Konno, T. Suzuki, T. Kitamura, T. Fujimoto, and T. Yoshida, Japanese J. of Appl. Phys. **57**, 065502 (2018)

[6] H. Fujikura, T. Konno, T. Kimura, Y. Narita, and F. Horikiri, Appl. Phys. Lett. **117**, 012103 (2020).

[7] T. Kimura, T. Konno, and H. Fujikura, Appl. Phys. Lett. **118**, 182104 (2021).

[8] Boccara A. C., Fournier D., Jackson W. B. and Amer N. M. Opt. Lett. **5** 377 (1980)

[9] M. Sumiya, S. Ueda, K. Fukuda, Y. Asai, Y. Cho, L. Sang, A. Uedono, T. Sekiguchi, O. Takeyoshi and T. Honda, Appl, Phys. Express **11**, 021002 (2018).

[10] M. Sumiya, D. Kindole, K. Fukuda, S. Yashiro, K. Takehana, T. Honda, Y. Imanaka, , Physica Status Solidi (B) Basic Research, 1900524, (2019).

[11] M. Sumiya, K. Fukuda, S. Takashima, S. Ueda, T. Onuma, T. Yamaguchi, T. Honda, A. Uedono, J. Crys. Growth **511**, 15 (2019).

[12] A. Uedono, S. F. Chichibu, Z. Q. Chen, M. Sumiya, R. Suzuki, T. Ohdaira; T. Mikado, T. Mukai, S. Nakamura, J. Appl. Phys. **90**, 181–186 (2001)

[13] W. B. Jackson and N. M. Amer, Phys. Rev. B **25**, 5559 (1982).

[14] A. Armstrong, A. Chakraborty, J. S. Speck, S. P. DenBaars, U. K. Mishra, S. A. Ringel, Appl. Phys. Lett. **89**, 262116 (2006).

[15] Nakano Y., Lozac'h M., Matsuki N., Sakoda K. and Sumiya M. 2011 J. Vac. Sci. Technol. B **29** 023001 (2011).

[16] E. Bustarret et al., J. of Non-Crys. Solids **77 & 78** (1985) 295–298.

[17] Y. Nakano, D. Ogawa, K. Nakamura, R. Kawakami, and M. Niibe, J. Vac. Sci. Technol. A 33, 043002 (2015).

[18] A. Armstrong, A. R. Arehart, and S. A. Ringel, J. Appl. Phys. **97**, 083529 (2005).

[19] K. C. Collins, A. M. Armstrong, A. A. Allerman, G. Vizkelethy, S. B. Van Deusen, F. Leonard, and A. A. Talin, J. Appl. Phys. **122**, 235705 (2017).

[20] A. Uedono, M. Imanishi, M. Imade, M. Yoshimura, S. Ishibashi, M. Sumiya, Y. Mori, J. Cryst. Growth **475** 261 (2017).

[21] Y. Mori. M. Imade, K. Murakami, H. Takazawa, H. Imabayashi, Y. Todoroki, K. Kitamoto, M. Maruyama, M. Yoshimura,Y. Kitaoka,T. Sasaki, J. Crys. Growth **350**, 72 (2012).

[22] A. Y. Polyakov; I.-H. Lee; N. B. Smirnov; A. V. Govorkov; E. A. Kozhukhova; S. J. Pearton, J. Appl. Phys. **109**, 123701 (2011)

[23] U. Honda, Y. Yamada, Y. Tokuda, and K. Shiojima, Jpn J. of Appl. Phys. **51**, 04DF04 (2012).

[24] In-Hwan Lee, A. Y. Polyakov, N. B. Smirnov, A. V. Govorkov, A. S. Usikov, H. Helava, Yu. N. Makarov, S. J. Pearton, J. Appl. Phys. **115**, 223702 (2014)

[25] 21A. Y. Polyakov, N. B. Smirnov, E. B. Yakimov, S. A. Tarelkin, A. V. Turutin, I. V. Shemerov, S. J. Pearton, K. Bin Bae, and I. H. Lee, J. Alloys Compd. **686**, 1044 (2016).

[26] K. Kanegae, M. Horita, T. Kimoto, and J. Suda, Appl. Phys. Express **11**, 071002 (2018)

[27] M. Sumiya, Jpn J. Appl. Phys. **62**, SN1007 (2023).

[28] E. Kioupakis, P. Rinke, A. Schleife, F. Bechstedt, and C. G. Van de Walle, Phys. Rev. B **81**, 241201 (2010).

[29] S. Pimputkar, S. Suihkonen, M. Imade, Y. Mori, J. S. Speck, S. Nakamura, J. Crys. Growth **432**, 49 (2015).

[30] O. Ambacher, W. Rieger, P. Ansmann, H. Angerer, T.D. Moustakas and M. Stutzmann, Solid State Commu. **97**, 365 (1996).

[31] Tran Thien Duc, Galia Pozina, Erik Janzen, and Carl Hemmingsson, J. Appl. Phys. **114**, 153702 (2013).

[32] K. Kanegae, H. Fujikura, Y. Otpki, T. Yoshida, M. Horita, T. Kimoto, and J. Suda, Appl. Phys. Lett. **115**, 012103 (2019).

[33] A. Y. Polyakov, I-H. Lee, N. B. Smirnov, A. V. Govorkov, E. A.Kozhukhova, S. J. Pearton, J. Appl. Phys. **109**, 12301 (2011).

[34] A. Y. Polyakov, N. B. Smirnov,A. V. Govorkov, T. G. Yugova, A. V. Markov, A. M. Dabiran, A. M. Wowchak, B. Cui; J. Xie; A. V. Osinsky; P. P. Chow; S. J. Pearton, Appl. Phys. Lett. **92**, 042110 (2008).

[35] D. W. Cardwell, A. Sasikumar, A. R. Arehart, S. W. Kaun, J. Lu, S. Keller, J. S. Speck, U. K. Mishra, S. A. Ringel, and J. P. Pelz, Appl. Phys. Lett. **102**, 193509 (2013).

[36] D. Wickramaratne, J.-X. Shen, C. E. Dreyer,M. Engel, M. Marsman, G. Kresse, S, Marcinkevičius, A, Alkauskas, and C. G. Van de Walle, Appl. Phys. Lett. **109**,162107 (2016).

[37] S. F. Chichibu, K. Shima, K. Kojima, S. Takashima, K. Ueno, M. Edo, H. Iguchi, T. Narita, K. Kataoka, S. Ishibashi and A. Uedono Jpn. J. of Appl. Phys. **58**, SC0802 (2019).